

# Synthesizing Majorana zero-energy modes in a periodically gated quantum wire

Mariana Malard<sup>1</sup>, George I. Japaridze<sup>2,3</sup>, and Henrik Johannesson<sup>4,5</sup>

<sup>1</sup>*University of Brasilia, 70904-910 Brasilia-DF, Brazil*

<sup>2</sup>*Ilia State University, Cholokasvili Ave. 3-5, 0162 Tbilisi, Georgia*

<sup>3</sup>*Andronikashvili Institute of Physics, Tamarashvili 6, 0177 Tbilisi, Georgia*

<sup>4</sup>*Department of Physics, University of Gothenburg, SE 412 96 Gothenburg, Sweden and*

<sup>5</sup>*Beijing Computational Science Research Center, Beijing 100094, China*

We explore a scheme for engineering a one-dimensional spinless  $p$ -wave superconductor hosting unpaired Majorana zero-energy modes, using an all-electric setup with a spin-orbit coupled quantum wire in proximity to an  $s$ -wave superconductor. The required crossing of the Fermi level by a single spin-split energy band is ensured by employing a periodically modulated Rashba interaction, which, assisted by electron-electron interactions and a uniform Dresselhaus interaction, opens a gap at two of the spin-orbit shifted Fermi points. While an implementation in a hybrid superconductor-semiconductor device requires improvements upon present-day capabilities, a variant of our scheme where spin-orbit-coupled cold fermions are effectively proximity-coupled to a BEC reservoir of Feshbach molecules may provide a ready-to-use platform.

PACS numbers: 74.78.Fk, 71.10.Pm, 03.67.Lx

## I. INTRODUCTION

The possible existence of an elementary fermionic particle with the distinguishing property of being its own antiparticle – a Majorana fermion – remains an outstanding puzzle, almost 80 years after the idea was first advanced<sup>1</sup>. By contrast, *emergent* Majorana fermions are well known to appear in disguise in condensed matter systems – the Bogoliubov quasiparticle in a superconductor being a notable example<sup>2,3</sup>.

Different, and more intriguing, is the concept of an emergent quasiparticle which is its own antiparticle but exhibits non-Abelian statistics<sup>4</sup> – a *Majorana zero-energy mode* (MZM), bound to a defect or a boundary<sup>5</sup>. Possible hosts for these particles are fractional quantum Hall systems<sup>6</sup>, cold gases of fermionic atoms<sup>7,8</sup> and topological superconductors in 1D<sup>9</sup> and 2D<sup>10,11</sup>. As first realized by Fu and Kane<sup>12</sup>, the required spinless  $p$ -wave pairing which makes a superconductor topological may be engineered in a semiconductor structure hybridized with an ordinary  $s$ -wave superconductor. This has made the topological superconductors the preferred hunting grounds for MZMs<sup>5</sup>, and there is now a variety of theoretical proposals for how to access them in the laboratory. Two schemes, both for proximity-induced 1D  $p$ -wave pairing, have so far been explored in experiments: A Rashba spin-orbit coupled quantum wire in proximity to an  $s$ -wave superconductor and subject to a magnetic field<sup>13,14</sup>, and a setup with a chain of magnetic impurities deposited on top of an  $s$ -wave superconductor<sup>15</sup>. While the experimental results are promising<sup>16</sup>, the verdict is still out as to whether any of them unambiguously points to MZMs.

To produce a topological superconducting state in one dimension, the basic trick is to make the Fermi level cross only a single spin-split quasiparticle band. With this, the pairing of the resulting helical (spin-momentum locked) states must then effectively have  $p$ -wave symmetry so as

to make the pair wave function antisymmetric<sup>9</sup>. In the quantum wire proposals of Refs. 13,14, the trick is carried out by combining a strong Rashba spin-orbit interaction (which causes the spin splitting) with a Zeeman interaction (which pushes one of the bands away from the Fermi level). In the more recent scenario with a magnetic impurity chain on top of an  $s$ -wave superconductor<sup>15</sup>, the microscopic spin texture of the chain emulates a combined Rashba and Zeeman interaction to effectively produce a protected set of one-dimensional  $p$ -wave states in the surface layer of the superconductor. While this latter setup has an advantage in allowing for STM probes of the predicted MZMs, it is more difficult to manipulate and control, and therefore probably less useful for future applications. The quantum wire setup, on the other hand, is easily controllable, with tunable gate voltages that may be used to move around the MZMs in networks of quantum wires – as envisioned in certain architectures for topological quantum gates<sup>17</sup>.

A potential problem of the quantum wire setup, however, is the reliance on a magnetic field. While the strength of the magnetic field can be varied, and allows to tune across the quantum phase transition from the ordinary to the topological superconducting phase – in this way uncovering experimental signatures of the MZMs – there are drawbacks: The presence of the field reduces the effectiveness of the proximity pairing by canting the spins<sup>18</sup>, and also makes the quantum wire setup less robust against disorder<sup>19,20</sup>. This is particularly damaging since a universal set of quantum gates<sup>21</sup> using MZMs is obtainable only by supplying ancillary nontopological states<sup>22,23</sup>. Nontopological states are prone to noise and disorder and, if assembled from 1D helical electron states, become even more fragile when subject to a magnetic field<sup>24</sup>. Moreover, magnetic fields of the required strengths are slow and hard to control locally<sup>25</sup>, and therefore, integrating them into useful designs for quantum computing with MZMs may prove ultimately un-

wieldy.

This raises the question whether MZMs may be produced in a quantum wire (or network of wires as required for braiding and quantum information processing) using an all-electric scheme, disposing of the magnetic field altogether. In fact, there is already an abundance of theoretical proposals which employ “non-magnetic” schemes:  $d_{x^2-y^2}$ <sup>26</sup> or  $s_{\pm}$ -wave proximity pairing<sup>27</sup>, noncentrosymmetric superconductivity<sup>28</sup>, two-channel quantum wires with channel-dependent spin-orbit interactions<sup>29</sup>, or some other mechanism<sup>30–38</sup>. Common to these proposals is that they describe time-reversal symmetric quasi-1D (“multichannel”) topological superconductors belonging to the DIII symmetry class<sup>39,40</sup>, hosting *paired* MZMs at each end of the wire (“Majorana Kramers pairs”)<sup>41</sup>. In this work we shall instead explore the possibility to generate *unpaired* MZMs at the ends of a truly 1D proximity-coupled quantum wire without applying a magnetic field, in this way realizing a magnetic-field-free 1D topological superconductor. Depending on whether time reversal symmetry is preserved or not, the effectively spinless  $p$ -wave superconductor thus obtained belongs to the BDI or D symmetry class<sup>41</sup>, respectively, with each case corresponding, in principle, to a different number of MZMs. We shall elaborate on both possibilities, finding that our setup always hosts a single unpaired MZM at each end of the wire, irrespective of whether time-reversal symmetry is broken or not. To the best of our knowledge, a scheme for producing unpaired MZMs without the use of a magnetic field has so far been discussed only for a model of a Floquet topological superconductor, with a periodic high-frequency driving of the spin-orbit interaction<sup>42</sup>. Here, we instead make use of a *spatially* periodic Rashba spin-orbit interaction.

Specifically, we shall build on a recent proposal of ours, where a helical system with spin-momentum-locked electrons is engineered using a quantum wire subject to a periodically modulated electric field<sup>43</sup>. The electric field gives rise to a spatially modulated Rashba spin-orbit interaction, which, when assisted by electron-electron (e-e) interactions and a uniform Dresselhaus spin-orbit interaction, opens a gap at two of the spin-orbit shifted Fermi points. As an outcome, a helical Luttinger liquid (HLL)<sup>44,45</sup> emerges at the two remaining gapless Fermi points. In the present work we inquire about the conditions under which the proximity of an ordinary  $s$ -wave superconductor could turn this HLL into a 1D spinless  $p$ -wave superconductor hosting MZMs. The problem becomes nontrivial considering that the induced superconducting pairing competes with the insulating gap-opening process from the modulated Rashba interaction. Using a perturbative renormalization-group argument, we shall find that both processes *can* play out concurrently. This establishes a “proof-of-concept” that a quantum wire may host unpaired MZMs without the assistance of a magnetic field (or a high-frequency driving of the spin-orbit interaction in time<sup>42</sup>). However, by feeding in realistic parameters for an InAs-based de-

vice into our theory, we find that the required strength of the modulated Rashba interaction lies outside the experimental range reported for the InAs quantum well. Possible routes to lower the value of the required Rashba coupling would be to increase the amplitude of the applied electric field, to enhance the proximity effect by improving the contacting in the hybrid device and to lower the temperature at which the experiment is carried out. A variant of our scheme with a cold-atom emulation of a quantum wire – where interacting and spin-orbit coupled fermionic atoms are in contact with a BEC reservoir of Feshbach molecules – looks quite promising. We shall elaborate also on this and argue that a spinless  $p$ -wave superfluid phase with unpaired MZMs is well supported by a cold atom platform within the parameter regime where our scheme is workable.

The paper is organized as follows. In the next section we introduce a microscopic model for a spin-orbit coupled and periodically gated quantum wire in proximity to an  $s$ -wave superconductor and advance, through general arguments, that this system may be turned into a spinless  $p$ -wave superconductor. As mentioned above, the scheme calls for the assistance of e-e interactions and this is discussed in Sec. III through a low-energy effective description of the model. Bosonizing the theory, we then carry out a detailed renormalization group study which allows us to establish the system’s phase diagram. In Section IV we identify the parameter regimes of the phase diagram, together with minimum practical conditions for sustaining the topological phase in the laboratory. The number of MZMs hosted by the topological superconductor and its possible symmetry classes are discussed in Section V. Finally, in Section VI, we present two case studies - one with a periodically gated InAs quantum wire and the other with an ultracold gas of optically trapped fermionic atoms - intended to assess the experimental viability of our scheme. Our conclusions are given in Section VII.

## II. SYNOPSIS: PHYSICAL PICTURE FROM THE MICROSCOPIC MODEL

In what follows we present and discuss the microscopic model that captures the physics of the system illustrated in Fig. 1: A quantum wire is gated by a periodic sequence of equally charged top gates and proximity coupled to an  $s$ -wave superconductor. The electrons in the wire are subject to e-e interactions and two types of spin-orbit interactions: the *Dresselhaus* and *Rashba* interactions. The Rashba coupling, being sensitive to an external electric field, will pick up the same modulation of the field from the electrodes. In addition, the chemical potential in the wire gets locally modulated by the electric array. Finally, the superconductor induces  $s$ -wave pairing in the wire through proximity effect.

To better understand the role of the various potentials introduced above, it is instructive to first consider a reduced system obtained by removing the  $s$ -wave pairing



lift the degeneracies at the center and at the boundaries of the reduced BZs, through hybridization of the  $+$  and  $-$  states. This is not so, however, since Kramers' theorem forces the  $+$  and  $-$  states to remain degenerate at the time-reversal invariant points  $k = 0$  and  $\pm k_r$ . So, while  $H_{so}$  will cause some distortion of the subbands in FIG. 2(b), the bands remain connected at  $k = 0, \pm\pi/3a$ .

The picture changes if time-reversal symmetry gets broken, either explicitly (by adding e.g. a magnetic field) or spontaneously. In this context, recall that strong to intermediate Umklapp scattering in a HLL causes a spontaneous breaking of time-reversal symmetry, with a concurrent opening of a gap in the spectrum<sup>44,45</sup>. As we shall demonstrate, time reversal symmetry similarly gets spontaneously broken when a Coulomb e-e repulsion

$$H_{e-e} = \sum_{n,n',\tau,\tau'} V(n-n') d_{n,\tau}^\dagger d_{n',\tau'}^\dagger d_{n',\tau'} d_{n,\tau} \quad (8)$$

is added to the Hamiltonian  $H = H_0 + H_{cp} + H_{so}$ .

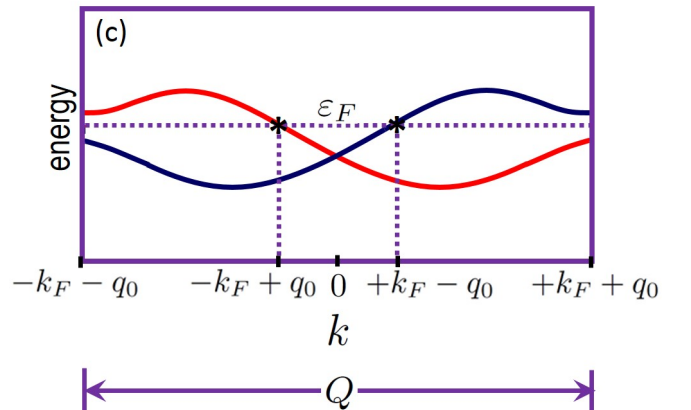
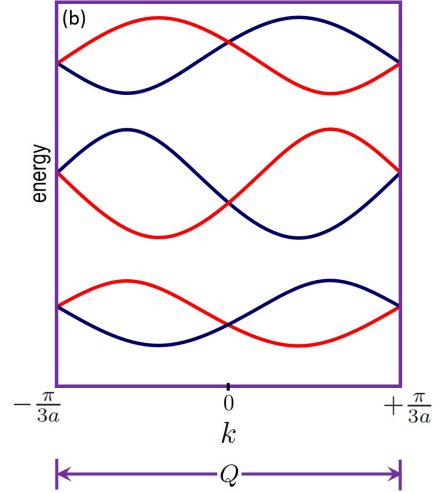
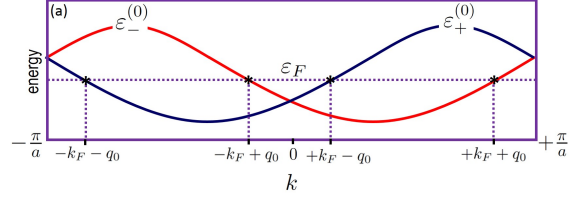
By inducing a spontaneous breaking of time-reversal symmetry in the wire, e-e interactions enable, in effect, the detachment of the bands at the boundaries of a reduced BZ. Specifically, in the next section we show that in the presence of e-e interactions, with the two outer Fermi points residing close to the boundaries of one of the reduced BZs such that  $|Q - 2(k_F + q_0)| \ll \mathcal{O}(1/a)$  (this will be the first reduced BZ if  $p = 1$ , the second if  $p = 2$ , etc.), then gaps open up at these boundaries, lifting the degeneracy of the the corresponding  $+$  and  $-$  states. As a result, the interior of this reduced BZ will support a HLL at the two remaining gapless Fermi points, with the  $\pm$  spin content of these states locked to the direction of motion of the electrons. FIG. 2(c) illustrates the case  $p = 1$  for which the lowest pair of bands of FIG. 2(b) develop gaps at the zone boundaries after inclusion of e-e interactions.

The effective “spinlessness” of the helical states in the interior of the reduced BZ implies that by incorporating into  $H = H_0 + H_{cp} + H_{so} + H_{e-e}$  an  $s$ -wave superconducting pairing potential of strength  $\Delta$ ,

$$H_{sc} = \sum_n [\Delta d_{n,+} d_{n,-} + \text{H.c.}], \quad (9)$$

may drive the system into a  $p$ -wave superconducting phase.

By means of this, the addition of e-e interactions in effect has triggered a quantum phase transition from an ordinary proximity-coupled  $s$ -wave superconductor to a topological spinless  $p$ -wave superconductor, with the “ $p$ -waveness” enforced by the antisymmetry of the pairing wave function that follows from the “spinless” nature of the helical states. It is interesting to note that this result is anticipated in a work by Stoudenmire *et al.*<sup>18</sup>, who hypothesized that a proximity-coupled quantum wire with strong Rashba and Dresselhaus couplings may be driven into a topological phase by interactions, even without an applied magnetic field. In the present work we provide the evidence that this is indeed possible.



The topological nontrivial character of a  $p$ -wave superconductor<sup>9</sup> implies that a finite wire, with the charging energy tuned to a degeneracy point<sup>49</sup>, can host localized MZMs  $\gamma_{L,i}$  and  $\gamma_{R,i}$ ,  $i = 1, 2, \dots, m$  at its left and right ends respectively. These modes, protected by chiral symmetry<sup>50</sup>, lead to a degenerate groundstate, up to small corrections from wave-function overlaps between left and right MZMs. Specifically, if  $|0\rangle$  is a ground state, then  $(\gamma_{L,i} + i\gamma_{R,i})|0\rangle$  is also a ground state, differing from the first by the presence of an extra electron. As we shall see, in the present case there is always only a single unpaired MZM ( $m = 1$ ) at each end of the wire.

Having outlined the backbone of our proposal, we close this section by stating the three basic conditions for it to work. First, the proximity gap must be smaller than the dynamically generated insulating gap at the zone boundaries, so that the states of the insulating and empty bands do not mix with the  $p$ -wave superconducting states. Secondly, the smaller proximity gap must itself exceed the thermal energy so that the device is robust against thermal leakage. Finally, the scaling lengths at which the gaps open up must fit within the system's cutoff length. The wire has to be sufficiently long also for suppressing the overlap between a left and right MZM wave function (which would otherwise produce a spectral weight for a finite-energy electronic mode). Let us note in passing that having a long wire alleviates the need to build in boundary- and finite-size effects into the description of the HLL. Thus our use of an infinite-volume formalism in what is to come. As we shall see, the conditions above can be given a precise mathematical formulation in the language of the perturbative renormalization group (RG). This and other key elements of the theory will be closely examined in what follows.

### III. LOW-ENERGY EFFECTIVE THEORY

To understand how the modulated spin-orbit interaction, e-e interactions and superconducting pairing team up to drive a phase transition from a trivial  $s$ -wave to a topological  $p$ -wave superconducting phase in the wire, we shall study the low-energy limit of the full Hamiltonian thus introduced,

$$H = H_0 + H_{cp} + H_{so} + H_{e-e} + H_{sc}, \quad (10)$$

with the terms defined in Eqs. (1)-(3), (8), and (9). We carry out this analysis in three steps: In subsection III.A, we linearize the spectrum around the system's four Fermi points in an extended zone picture, with that producing an effective field theory written in terms of fermionic right- and left-moving field operators. A bosonization procedure is applied in subsection III.B, casting the theory in a form that will be analyzed within an RG formalism in subsection III.C.

#### A. Linearization of the spectrum

To fix a working ground (without loss of generality), let us consider the lowest bands of FIG. 2(b). Using a low-energy approach, we will show how these bands can be evolved into the partially gapped band structure depicted in FIG. 2(c). The first step is to choose the Fermi level so that the outer Fermi points  $\pm k_F \pm q_0$  reside in the neighborhoods of the boundaries of the first reduced BZ, so that  $|Q - 2(k_F + q_0)| \ll \mathcal{O}(1/a)$ . (For ease of exposition we put  $Q = 2(k_F + q_0)$  in the following. However, all results obtained in the continuum limit remain valid as long as  $|Q - 2(k_F + q_0)| \ll \mathcal{O}(1/a)$ .) Here it is important to note that the modulation wave number  $Q$  is likely to be preset in an experimental device. Thus, rather than choosing  $Q$ , it is instead  $k_F$  that is tuned – by filling up the system via a backgate – so as to make the outer Fermi points approach the zone boundaries.

Having thus defined the Fermi level, the next step is to linearize the spectrum around the four Fermi points  $\pm k_F + \tau q_0$  ( $\tau = \pm$ ). This calls for an extended zone scheme that takes advantage of translational symmetry to formally “disentangle” the bands at the boundaries of the reduced BZ. This scheme is represented in FIG. 3(a)-(b): the enclosed pieces of the  $+$  and  $-$  bands are displaced by the reciprocal vector  $Q$ , rendering two parabolic-like bands in the extended zone scheme. With this, the linearization of the spectrum, as illustrated in FIG. 3(c), can be carried out in the standard way.

The continuum limit of the low-energy (linearized) theory is obtained through the transformations  $na \rightarrow x$ ,  $\sum_n \rightarrow \int dx/a$  and

$$d_{n,\tau} \rightarrow \sqrt{a}(e^{i(k_F + \tau q_0)x} R_\tau(x) + e^{i(-k_F + \tau q_0)x} L_\tau(x)),$$

where  $R_\tau(x)$  and  $L_\tau(x)$  are fermionic field operators that annihilate right- and left-moving excitations at the respective Fermi points. Specifically,  $L_-$  and  $R_+$  apply to the “outer” Fermi points  $-k_F - q_0$  and  $+k_F + q_0$  respectively, while  $L_+$  and  $R_-$  apply to the “inner” ones,  $-k_F + q_0$  and  $+k_F - q_0$  respectively.

Omitting rapidly oscillating terms that vanish upon integration when  $Q = 2(k_F + q_0)$ , we find that  $H \rightarrow \int dx (\mathcal{H}_{outer} + \mathcal{H}_{inner} + \mathcal{H}_{e-e})$  where

$$\begin{aligned} \mathcal{H}_{outer} = & -iv_F (:R_+^\dagger \partial_x R_+ : - :L_-^\dagger \partial_x L_- :) \\ & + \lambda (R_+^\dagger \partial_x L_- + L_-^\dagger \partial_x R_+) \end{aligned} \quad (11)$$

$$\begin{aligned} \mathcal{H}_{inner} = & -iv_F (:R_-^\dagger \partial_x R_- : - :L_+^\dagger \partial_x L_+ :) \\ & + \Delta (R_-^\dagger L_+^\dagger + L_+ R_-), \end{aligned} \quad (12)$$

$$\begin{aligned} \mathcal{H}_{e-e} = & \sum_{\tau, \tau'} g_1 : R_\tau^\dagger L_\tau L_{\tau'}^\dagger R_{\tau'} : + g_2 : R_\tau^\dagger R_\tau L_{\tau'}^\dagger L_{\tau'} : \\ & + \frac{g_2}{2} (:L_\tau^\dagger L_\tau L_{\tau'}^\dagger L_{\tau'} : + L \rightarrow R), \end{aligned} \quad (13)$$

with  $v_F = 2a\tilde{t}\sin(k_F a)$ ,  $\lambda = a\gamma'_R\gamma_D/\gamma_{eff}$ ,  $g_1 \sim \tilde{V}(k \sim 2k_F)$ ,  $g_2 \sim \tilde{V}(k \sim 0)$ ,  $\tilde{V}(k)$  being the Fourier transform of

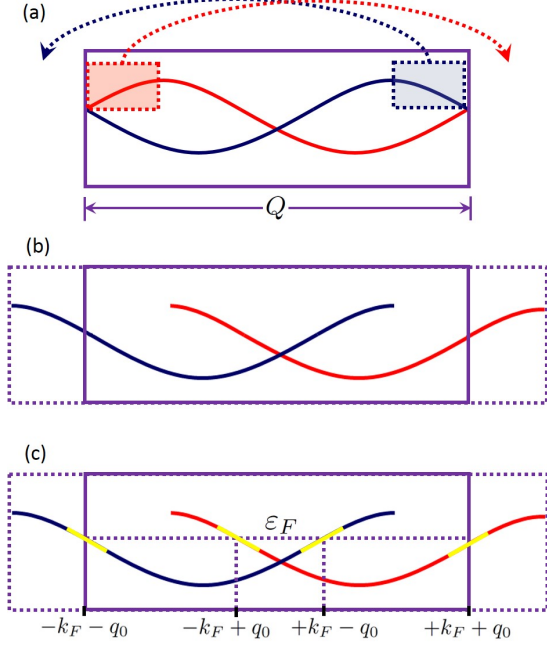


FIG. 3: (a) Energy + and - bands with boxed segments being displaced by a reciprocal vector. (b) Resulting spin-split parabolic-like bands in the extended zone scheme. (c) Linearization of the spectrum around the Fermi level.

the Coulomb potential, and where  $\dots$  denotes normal ordering. The backscattering process  $\sim g_1$  is known to be RG irrelevant in a Luttinger liquid<sup>51</sup>, and the same holds true in the presence of spin-orbit interactions and superconducting pairing<sup>52</sup>. Here we thus consider only the dispersive and forward scattering processes  $\sim g_2$  in Eq. (13).

### B. Bosonized theory

The physics of Eqs. (11)-(13) reveals itself in a more transparent way if we go to a bosonized picture by applying the prescription<sup>51</sup>:

$$R_\tau = \frac{\eta_\tau^R}{\sqrt{2\pi a}} e^{-i\sqrt{\pi}(\phi_i + \tau\theta_i)}, \quad (14)$$

$$L_\tau = \frac{\eta_\tau^L}{\sqrt{2\pi a}} e^{+i\sqrt{\pi}(\phi_j + \tau\theta_j)}, \quad (15)$$

where  $i = 1$  (2) applies to  $\tau = +$  ( $-$ ) and  $j = 1$  (2) applies to  $\tau = -$  ( $+$ );  $\phi_i(x)$  and  $\theta_i(x)$  are dual bosonic fields satisfying  $v_F \partial_x \theta_i = \mp \partial_x \phi_i$  (with  $i = 1$  (2) for the minus (plus) sign), and  $\eta_\tau^{R,L}$  are the Klein factors needed to preserve the Fermi statistics of the  $R_\tau$  and  $L_\tau$  fields.

The bosonized Hamiltonian reads  $H = \int dx (\mathcal{H}'_{outer} + \mathcal{H}'_{inner} + \mathcal{H}_{mix})$  with

$$\begin{aligned} \mathcal{H}'_{outer} = & u[(\partial_x \theta_1)^2 + (\partial_x \phi_1)^2] - \frac{\Delta}{\pi a} \sin(\sqrt{\frac{4\pi}{K}} \theta_1) \\ & + \frac{\lambda}{\sqrt{\pi K} a} \cos(\sqrt{4\pi K} \phi_1) \partial_x \theta_1, \end{aligned} \quad (16)$$

$$\mathcal{H}'_{inner} = u[(\partial_x \theta_2)^2 + (\partial_x \phi_2)^2] - \frac{\Delta}{\pi a} \sin(\sqrt{\frac{4\pi}{K}} \theta_2), \quad (17)$$

$$\mathcal{H}_{mix} = \frac{g_2 K}{\pi} \partial_x \phi_1 \partial_x \phi_2, \quad (18)$$

where  $K = (1 + g_2/(\pi v_F))^{-1/2}$  is the Luttinger parameter, and  $u = v_F/2K$  is the Fermi velocity dressed by e-e interactions. The non-interacting limit corresponds to  $K = 1$  (i.e.  $g_2 = 0$ ), for which  $\mathcal{H}_{mix} = 0$ , and, referring back to Eqs. (11) and (12),  $\mathcal{H}'_{outer} = \mathcal{H}_{outer}$  and  $\mathcal{H}'_{inner} = \mathcal{H}_{inner}$ . The bosonized theory is thus seen to split into two branches given by  $\mathcal{H}'_{outer}$  and  $\mathcal{H}'_{inner}$ , each acting at the corresponding pair of outer and inner Fermi points, and, for  $K \neq 1$ , coupled by the Hamiltonian term  $\mathcal{H}_{mix}$ .

In Ref. 43 we analyzed the bosonized theory defined by Eqs. (16)-(18) in the absence of superconducting pairing, i.e. with  $\Delta = 0$ . Going to a path integral formulation, we found that by integrating out the last term in Eq. (16), the outer branch gets described by a quantum sine-Gordon model with potential  $\propto \lambda^2 \cos(\sqrt{16\pi K} \phi_1)$ . This potential is strongly RG-relevant if  $K < 1/2$  (strong e-e repulsion). If  $K \geq 1/2$  (weak e-e repulsion), it is marginally RG-relevant provided the strength  $\lambda$  of the modulated spin-orbit interaction is sufficiently large, satisfying  $(\lambda/v_F)^2 > (2 - 1/K)^{53}$ . In both cases, the term opens a gap for the electrons in the outer branch, at the same time as it suppresses the branch-mixing term in Eq. (18) by pinning the  $\phi_1$ -field. As a result, the inner branch decouples and comes to support an HLL. Folding back the extended zone into the first reduced BZ, we arrive at the gapped band structure anticipated in FIG. 2(c). If  $K \geq 1/2$  but  $(\lambda/v_F)^2 \leq (2 - 1/K)$ , the spin-orbit potential becomes RG-irrelevant, the bands remain gapless, and the system an ordinary Luttinger liquid.

The HLL put forward in Ref. 43 is different from the ones that have so far been studied experimentally: It is neither holographic<sup>54</sup> (unlike the edge states of a quantum spin Hall insulator) nor quasihelical<sup>55</sup> (unlike a magnetic-field-assisted helical liquid). The time-reversal analog of the fermion-doubling problem implied by Kramers' theorem<sup>54</sup> is instead avoided by the fact that the gapped branch breaks time-reversal symmetry



*spontaneously* by developing a spin-density wave (SDW). This can be seen from an analysis in Ref. 44, which, when carried over to  $\mathcal{H}'_{outer}$  in Eq. (16) with  $\Delta = 0$ , reveals that the Ising-like SDW operator  $i(R_+^\dagger L_- - \text{H.c.}) \sim \cos(\sqrt{4\pi}\phi_1)$  takes on a finite expectation value in the gapped ground state (due to the pinning of the  $\phi_1$ -field)<sup>43</sup>. It is important to point out that this spontaneous breaking of time reversal symmetry (that enables the modulated spin-orbit interaction to gap out one branch, isolating a HLL in the other) is only possible in the presence of sufficiently strong e-e interactions. If the interaction is weak ( $K \approx 1$ ), a pinning of  $\phi_1$  would require the marginal RG-flow to be launched from an impracticably high point in the  $K-\lambda$  plane with  $\lambda > \sqrt{2}v_F$ .

Let us now consider the effect of the superconducting pairing. Switching on the pairing field  $\Delta$ , the inner branch acquires a sine-Gordon term as given by Eq. (17). This perturbation is strongly RG-relevant if  $K > 1/2$  (weak e-e repulsion), while if  $K \leq 1/2$  (strong e-e repulsion) it is marginally relevant provided the strength  $\Delta$  of the superconducting pairing is enough to survive the e-e repulsion, satisfying  $a\Delta/v_F > (1/K - 2)$ . In both cases, a superconducting gap opens up in the inner branch. If, on the other hand,  $K \leq 1/2$  with  $a\Delta/v_F \leq (1/K - 2)$ , the superconducting pairing gets suppressed by strong e-e repulsion, becoming RG-irrelevant.

One can now envision that combining a (strongly or marginally) relevant superconducting pairing in the inner branch with a (strongly or marginally) relevant spin-orbit interaction in the outer branch, the *s*-wave coupled helical electrons will undergo a transition to a *p*-wave topological phase. Because the outer branch is now also subject to a superconducting pairing (see Eq. (16)), the regime of parameters for which this phase transition takes place depends on how superconductivity and spin-orbit coupling play out together in that branch. Specifically, one asks whether there is a parameter regime in which the insulating order in the outer branch dominates superconducting pairing correlations, and hence makes possible the emergence of an HLL in the inner branch (thus preconditioning the appearance of the topological superconductor).

To find out we proceed to investigate the theory given by Eq. (16). It is here important to note that if this theory does support an insulating phase, then, within this phase, the mixing term in Eq. (18) is killed by the pinning of the  $\phi_1$ -field and the outer and inner branches decouple.

### C. Renormalization Group analysis of the outer branch

To investigate the theory given by Eq. (16) it is convenient to go to a Lagrangian formalism. After carrying out a Legendre transformation of Eq. (16), and integrating out the conjugated momentum field  $\Pi_1 = -\partial_x \theta_1$  from the partition function, we arrive at the effective action

for the outer branch:

$$S_{outer} = \int dx d\tau \left[ \frac{2u}{2} \left( (\partial_x \phi_1)^2 + \frac{1}{(2u)^2} (\partial_\tau \phi_1)^2 \right) - \frac{v_F g_{so}}{\pi a^2} \cos(\sqrt{16\pi K} \phi_1) - \frac{v_F g_{sc}}{\pi a^2} \cos\left(\sqrt{\frac{4\pi}{K}} \theta_1\right) \right], \quad (19)$$

where  $\tau = it$  is the imaginary time and where  $g_{sc} = a\Delta/v_F$  and  $g_{so} = \lambda^2/(4v_F^2)$  are dimensionless coupling constants.

The Action (19) is an extended version of the sine-Gordon model where, besides the usual mass term given by the cosine of the  $\phi_1$ -field, a cosine of the dual  $\theta_1$ -field is also present. This model has been a subject of intensive studies during the past decades<sup>56–58</sup>. We note the manifest invariance of Eq. (19) under the duality transformation  $\phi_1 \leftrightarrow \theta_1$  and  $2K \leftrightarrow 1/(2K)$ , i.e. the property of a self-dual sine-Gordon model if  $g_{so} = g_{sc}$ . For details we refer the reader to the Ref. [59].

A crucial feature of the model described by Eq. (19) is that its two cosine potentials are mutually nonlocal and, therefore, cannot be minimized simultaneously. Although the strengths (bare masses)  $g_{so}$  and  $g_{sc}$  of these two cosines are determined by interactions of different origins (spin-orbit interaction and superconducting pairing, respectively), the respective scaling dimensionalities  $\Delta_{so} = 4K$  and  $\Delta_{sc} = 1/K$  are controlled by the same parameter  $K$  (that is, by e-e interactions). Since  $\Delta_{so}\Delta_{sc} = 4$ , either one of the cosine perturbations is strongly relevant when its scaling dimensionality is less than 2, else the perturbation is irrelevant or marginally relevant. Thus,  $K < 1/2$  implies a strongly relevant  $g_{so}$ -perturbation and an irrelevant or marginally relevant  $g_{sc}$ -perturbation, with the complementary conclusion for  $K > 1/2$ . The case  $K = 1/2$  corresponds to both interactions being marginally relevant.

When one of the perturbations is strongly relevant and the other is irrelevant, the low-energy physics of the model is simply governed by the strongly relevant operator and the problem effectively reduces to the standard sine-Gordon model, either for the  $\phi_1$ -field when  $K < 1/2$  or for the  $\theta_1$ -field when  $K > 1/2$ . In this case the resulting infrared theory is fully massive and the continuous translational symmetry of the free gapless Gaussian model is broken down to the discrete  $Z_N$  symmetry associated with the minima of the strongly relevant cosine. The corresponding field becomes pinned in one of these minima. In the case of the  $g_{so}$ -perturbation, the symmetry breaking is translated into an insulating order sustained by a dynamically generated soliton gap<sup>59</sup>, whereas for the  $g_{sc}$ -perturbation, the symmetry breaking is translated into a superconducting order sustained by a pairing gap.

The most interesting situations arise (i) when one of the perturbations is strongly relevant and the other is marginally relevant (according to a straightforward dimensionality analysis) but with both having scaling dimensionality close to 2 (implying  $K \approx 1/2$ ) and (ii) when

both perturbations are marginally relevant and have scaling dimensionalities exactly equal to 2 (at  $K = 1/2$ ). In these cases, the self-duality opens a possibility for the existence of a critical point (or line) separating two regimes, each governed by one of the antagonistic  $g_{so}$ - and  $g_{sc}$ -terms<sup>58</sup>. The outcome of the competition between the corresponding self-excluding orders depends not only on the parameter  $K$  but also on the relation between the corresponding energy scales  $g_{so}$  and  $g_{sc}$ .

To uncover this process in detail, we exploit the perturbative RG solution of the model given by Eq. (19) in the neighborhood of the Gaussian fixed point  $K = 1/2$ , obtained using an operator product expansion of the S-matrix<sup>59</sup>. Defining the electron-electron interaction parameter  $g_{ee}$  through  $K = 1/2 - g_{ee} + O(g_{ee}^2)$ , the RG flow equations for  $g_{ee}$ ,  $g_{so}$  and  $g_{sc}$  can be read off from the one-loop expansion carried out in Ref. 59:

$$\frac{dg_{ee}}{dl} = g_{so}^2 - g_{sc}^2, \quad (20)$$

$$\frac{dg_{so}}{dl} = 4g_{so}g_{ee}, \quad (21)$$

$$\frac{dg_{sc}}{dl} = -4g_{sc}g_{ee}, \quad (22)$$

where  $l = \ln s$ , with  $s$  a scale factor.

By numerically solving these equations we obtain the RG flows  $g_{ee}(l)$ ,  $g_{so}(l)$  and  $g_{sc}(l)$  of the corresponding parameters in the outer branch. FIG. 4 displays the flows for nine different sets of  $g_{ee}$ ,  $g_{so}$  and  $g_{sc}$  bare ( $l = 0$ ) values. Here it is instructive to note that the bare values  $g_{ee}$  (or  $K$ ) and  $g_{sc}$  (or  $\Delta$ ) are common to both the outer and inner branches as these are values determined by the microscopic parameters of the system. However, the RG flows of these parameters in the outer and inner branches are independent since these branches are subject to different perturbations. The initial values shown in FIG. 4 are test numbers chosen so that the inner branch is ensured to be in the superconducting phase ( $K > 1/2 \Rightarrow g_{ee} < 0$ ).

FIG. 4 shows that the phase diagram of the outer branch consists of a superconducting phase and an insulating phase separated by a critical plane which is the locus of the theory's fixed points. The plane equation obtained from the numerics

$$g_{so} - g_{sc} + 2g_{ee} = 0 \quad (23)$$

can also be derived analytically, as shown in Ref. 59. For initial values of the parameters corresponding to a point on the plane, the resulting flow will be constrained to the plane, eventually sticking to a fixed point.

Below the plane, the spin-orbit interaction becomes irrelevant and the superconducting pairing relevant. As a result, a pairing gap opens in the outer branch, leading to a superconducting phase. More interesting, for the realization of our scheme, is the region above the

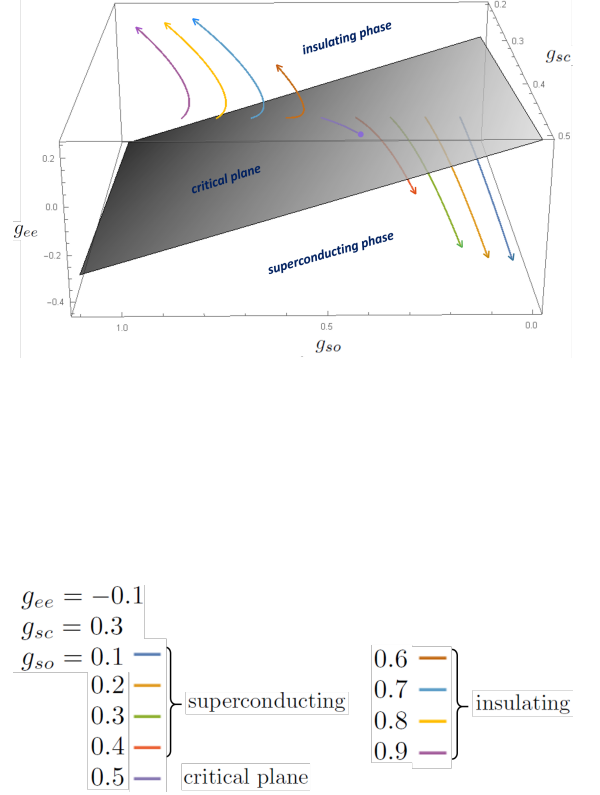


FIG. 4: (Color online) RG phase diagram obtained by numerical solution of the flow equations (20)-(22). The critical plane equation is:  $g_{so} - g_{sc} + 2g_{ee} = 0$

critical plane. Here superconducting pairing goes irrelevant, while the spin-orbit potential becomes relevant. It follows that an insulating gap opens up, sustaining an insulating phase above the plane.

The next step is to determine the regime of parameters in which the topological superconducting phase arises by combining the conditions for insulating order in the outer branch and superconducting order in the inner branch. Besides, some minimum practical criteria must be met so as to sustain the topological phase in the laboratory. These issues will be addressed in the next section.

#### IV. PARAMETER REGIMES

Rewritten in terms of the parameters  $g_{ee}$  and  $g_{sc}$ , the regimes discussed in Sec. III.B for the inner branch are: (inner-1) irrelevant superconducting pairing when  $g_{ee} \geq 0$  and  $g_{sc} \leq \sqrt{2}g_{ee}$ ; (inner-2) marginally relevant pairing when  $g_{ee} \geq 0$  and  $g_{sc} > \sqrt{2}g_{ee}$ ; and (inner-3)



strongly relevant pairing when  $g_{ee} < 0$ . On the other hand, the analysis carried out in Sec. III.C showed that the outer branch admits two regimes: (outer-1) relevant superconducting pairing (with irrelevant spin-orbit interaction) when  $g_{so} - g_{sc} + 2g_{ee} < 0$ , and (outer-2) relevant spin-orbit interaction (with irrelevant pairing) when  $g_{so} - g_{sc} + 2g_{ee} > 0$ . Combining these conditions, we arrive at the regimes of parameters that comprise the full phase diagram of the system:

- $SWS = \{g_{sc} > 2g_{ee} + g_{so}\}$
- $HLL = \{g_{ee} \geq 0, g_{sc} \leq \sqrt{2}g_{ee}\}$
- $PWS_1 = \{g_{ee} \geq 0, \sqrt{2}g_{ee} < g_{sc} < 2g_{ee} + g_{so}\}$
- $PWS_2 = \{g_{ee} < 0, g_{sc} < 2g_{ee} + g_{so}\}$

with  $SWS$  standing for  $s$ -wave superconductor,  $HLL$  for helical Luttinger liquid and  $PWS$  for  $p$ -wave superconductor.

Now, although necessary, the condition that the parameters belong to one of the regimes  $PWS_1$  or  $PWS_2$  is not sufficient to guarantee a “working” topological superconductor. The corresponding conditions on the parameters must be supplemented by at least three “practical” criteria:  $PC_1$  - The insulating gap must exceed the superconducting gap, otherwise it becomes energetically favorable to open a superconducting gap at all four Fermi points, losing the  $p$ -wave state. This parallels the condition that the Zeeman gap in the more conventional scheme for obtaining a 1D spinless  $p$ -wave superconductor in a quantum wire must be larger than the proximity gap<sup>5</sup>;  $PC_2$  - The superconducting gap itself must exceed the thermal energy  $k_B T$  at lab temperatures  $T$ , so as to withstand thermal leakage;  $PC_3$  - The physical scaling lengths at which the gaps open up (in the language of RG<sup>51</sup>) must not exceed the system’s cutoff length for the gap opening processes to effectively come into play. In the case of a defect and impurity-free system (realizable in a cold-atom emulation of a quantum wire, cf. Sec. VI.B), the cutoff length is the system’s size  $Na$ , while for a quantum wire in a semiconductor heterostructure with electron-impurity scattering, it will be the localization length  $L_{loc}$ .

The superconducting gap  $M_{sc}$  and the insulating gap  $M_{ins}$  can be computed from the general expression<sup>51</sup>

$$M = \Lambda e^{-l^*}, \quad (24)$$

where  $M$  is the gap,  $\Lambda$  is the RG energy cutoff and  $l^*$  is the RG scaling length at which the gap opens up, that is, the dimensionless length at which the coupling  $-g_{sc}$  or  $g_{so}$  becomes of order unity; call it  $l_{sc}^*$  for  $M_{sc}$  and  $l_{ins}^*$  for  $M_{ins}$ .

The physical dimensionful scaling length  $L$  at which a gap opens is obtained from the corresponding RG scaling length  $l^*$  via:

$$L = a e^{l^*}. \quad (25)$$

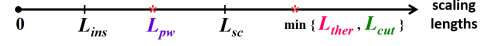


FIG. 5: (Color online) The scaling lengths  $L_{sc}$  and  $L_{ins}$  at which the superconducting and insulating gaps, respectively, open up and their corresponding upper bonds  $\min\{L_{ther}, L_{cut}\}$  and  $L_{pw}$  for an observable  $p$ -wave topological phase.

Using eqs. (24) and (25), the practical criteria  $PC_1$ ,  $PC_2$  and  $PC_3$  translate into:

- $PC_1 : L_{ins} < L_{pw}$
- $PC_2 \& PC_3 : L_{sc} < \min\{L_{ther}, L_{cut}\}$

where the length  $L_{pw} \equiv L_{sc}/r$ , with  $r \geq 1$ , is the upper bond on  $L_{ins}$  above which the  $p$ -wave state is lost;  $L_{ther} \equiv \Lambda a/(k_B T)$  is a thermal length such that if  $L_{sc} > L_{ther}$  thermal energy starts to destroy the superconducting pairing in the inner branch and, with increasing temperature, also the insulating state in the outer branch; and  $L_{cut} \equiv Na(L_{loc})$  is the system’s cutoff length for a defect and impurity-free system (quantum wire with electron-impurity scattering). FIG. 5 summarizes the practical criteria above.

Having established the regime of parameters of an observable  $p$ -wave superconducting phase, we next present an analysis of the symmetry classes and number of MZMs associated with this topological phase.

## V. SYMMETRY CLASSES AND NUMBER OF UNPAIRED MAJORANA ZERO MODES

As detailed in the previous section, the emergence of a topological superconducting phase in the inner branch - preconditioned by a decoupling of the inner and outer branches in Eqs. (16)-(18) - requires that the e-e interaction parameter  $g_{ee}$  takes a value inside the  $PWS_1$  or inside the  $PWS_2$  regime. As a Gedankenexperiment, however, let us temporarily remove the outer branch from the problem entirely, allowing for the emergence of a spinless  $p$ -wave superconducting phase for any value  $g_{ee} < 0$ , that is for any  $K > 1/2$ , for which the pairing potential in Eq. (17) is strongly RG-relevant. It is then instructive to consider the noninteracting case,  $K = 1$ , for which the

effective theory in Eq. (17) is simply the bosonized version of the fermionic Hamiltonian  $\mathcal{H}_{inner}$  in Eq. (12). This fermionic theory has a linearized spectrum, and, as concerns its topological properties, does not easily fit into the usual topological classification scheme<sup>39,40</sup> since the unboundedness of its spectrum makes the  $k$ -space topology fuzzy. While a Hamiltonian with a linearized spectrum around the Fermi points may still allow for the identification of differences in the winding numbers which define the 1D topological invariants for different parametrizations<sup>60,61</sup>, it does not *per se* provide information about e.g. the number of end-MZMs. For this one needs a Bogoliubov-de Gennes (BdG) Hamiltonian defined on the full Brillouin zone. In other words, the number of unpaired MZMs hosted by  $\mathcal{H}_{inner} + \mathcal{H}_{e-e}$  when  $\mathcal{H}_{outer}$  is gapped out can only be deduced from the full underlying theory which exhibits the topological phase. However, in the present case we do not know this theory since the possible topological phase is generated dynamically, and - within our approach - can be accessed only by going to an effective low-energy description with a linearized spectrum. To evade this quagmire we take resort to a construction that connects our low-energy effective theory to an auxiliary theory with a well-defined topological invariant.

For this purpose, let us consider the Hamiltonian which describes, in the full Brillouin zone, a 1D spinless  $p$ -wave superconductor:

$$H_p = \int dx \psi \left( -\frac{\partial_x^2}{2m} - \mu \right) \psi - \Delta_p \psi \left( \frac{i\partial_x}{k_F} \right) \psi + \text{H.c.}, \quad (26)$$

where  $\psi$  is a spinless fermion field,  $m$  is an effective mass,  $\mu$  is the chemical potential, and  $\Delta_p$  is the  $p$ -wave pairing potential. By linearizing the spectrum of the theory described by Eq. (26) for  $\mu > 0$  and writing  $\psi(x) = e^{ik_F x} R_+(x) + e^{-ik_F x} L_-(x)$ , using that to leading order  $-i\psi(x)\partial_x\psi(x) \approx 2L(x)R(x)$  (and dropping RG irrelevant terms and terms which fluctuate fast and average to zero upon integration),  $H_p$  in Eq. (26) gets mapped onto  $\int dx \mathcal{H}_{inner}$ , with  $\mathcal{H}_{inner}$  given in Eq. (12) and  $\Delta \approx 2\Delta_p$ . An analysis of the BdG Hamiltonian corresponding to  $H_p$  shows that its band structure has topological winding number  $W = 1$  for  $\mu > 0$  and  $\Delta$  real-valued<sup>50</sup>, implying that each end of the wire hosts a single unpaired MZM. Through the mapping above, the same conclusion can be extended to  $\mathcal{H}_{inner}$  with an added e-e interaction provided that the superconducting gap remains finite since, in this case, the unpaired MZMs are known to be stable against e-e interactions<sup>18,62,63</sup>. It follows that if we reverse the procedure and start with a linearized 1D theory supporting a superconducting phase *with* e-e interactions, this phase can be smoothly connected to the noninteracting 1D  $p$ -wave superconductor in Eq. (26) with well-defined topological properties: Inside the regimes  $PWS_1$  and  $PWS_2$ , the e-e interaction is constrained to a “window of opportunity” so as to stabilize the system of  $s$ -wave paired helical electrons in an effectively spinless  $p$ -wave topological phase. This estab-

lishes that our scheme is capable of producing a single unpaired MZM at each end of the wire.

The discussion above assumed that the pairing field in Eq. (26) is constant, with a complex phase which can be gauged away. This puts the topological superconductor in the BDI symmetry class<sup>50</sup>, where the  $\mathbb{Z}$  topological invariant is calculated as a winding number  $W$  which counts the number of unpaired end-MZMs. However, the appearance of a SDW in the outer insulating branch (cf. Sec. III.B) may possibly act as a dynamically generated staggered magnetic field in the topological sector, inducing a phase gradient in the pairing field which cannot be gauged away. The resulting spontaneous breaking of time-reversal symmetry in the inner branch would then change the symmetry class to D<sup>64</sup>, with a  $\mathbb{Z}_2$  topological invariant taking the value unity when  $\mu > 0$ . As before, this implies a single unpaired end-MZM. So, although our formalism is not sufficiently powerful to decide whether or not time reversal is spontaneously broken also in the inner branch, the issue is immaterial to our objective to show the emergence of MZMs. In either case, with (or without) symmetry breaking in the inner branch, the D (BDI) symmetry class (with  $W = 1$ ) rules that there will be a single unpaired MZM at each end of the wire.

Although not important for our study, one should still keep in mind that the  $\mathbb{Z}$  topological invariant of a 1D noninteracting BDI phase gets broken down to  $\mathbb{Z}_8$  in presence of interactions, leaving eight distinct equivalence classes<sup>65,66</sup> that can be matched to eight of the ten Altland-Zirnbauer symmetry classes<sup>67</sup>. While a vital result which highlights the shortcoming of topological band theory for interacting systems, we bypass it by showing that the underlying auxiliary theory without interactions,  $H_p$  in Eq. (26), has a topological winding number with value unity, implying single unpaired end-MZMs for which we can then refer to the stability analyses carried out in Refs. 18,62,63.

Next, we will attach experimental values to the parameters in order to evaluate the viability of our proposal in light of the theoretical and practical criteria established in Sec. IV. We present two case studies: a quantum wire in a semiconductor quantum well and a quantum wire made of cold atoms trapped in an optical lattice.

## VI. CASE STUDIES

### A. Case study I: InAs quantum wire

As a first case study, we investigate the setup of Fig. 1 with the quantum wire patterned in an InAs quantum well (QW).

Starting with  $PC_2$  &  $PC_3$ , we may write  $L_{therm} = \Lambda a / (k_B T) = \hbar v / (k_B T)$ , with  $v$  the drift velocity of the electrons in the semiconductor QW. Using  $v \approx 10^5$  m/s<sup>68</sup> and  $T \approx 0.1$  K, which is well above the low temperatures at which the experimental searches for MZMs have been carried out<sup>69-71</sup>, we get  $L_{therm} \approx 7.6 \mu\text{m}$ . We expect

$L_{loc} \approx 10 \mu\text{m}$ , guided by a prediction by Liu and Das Sarma<sup>72</sup> that the localization length in a high-quality GaAs quantum wire can be several microns long, and using that the electron mobility in an InAs wire is at least 5 times larger than that of a GaAs wire<sup>73</sup>. Thus,  $PC_2 \& PC_3$  demands that  $L_{sc} \lesssim 7.6 \mu\text{m}$ . Using Eq. (25) with  $a \approx 5 \text{ \AA}$ <sup>68</sup>, the previous condition can be written in terms of the corresponding dimensionless RG scaling length as  $l_{sc}^* \lesssim 9.6$ . It remains to check whether this condition is experimentally attainable.

We start by fixing the bare value of the superconducting pairing parameter  $g_{sc}$  by assuming a proximity effect in the upper range of what has so far been reported from experiments. Recalling that  $g_{sc} = a\Delta/(\hbar v)$  and taking  $\Delta \approx 3.5 \text{ K}$  - corresponding to the estimated zero-field proximity gap in an InSb-NbTiN hybridized device<sup>69</sup> - gives (with the same values for  $a$  and  $v$  as above)  $g_{sc} \approx 2.3 \times 10^{-3}$ . We then ask what is the range for the e-e parameter  $g_{ee}$  so that the RG flow of  $g_{sc}$  reaches unity at a scaling length  $l_{sc}^* \lesssim 9.6$  when the bare  $g_{sc} \approx 2.3 \times 10^{-3}$ . From the numerics, we find that  $-0.50 \leq g_{ee} \lesssim -0.20$ .

Recalling that  $g_{ee} \equiv 1/2 - K$ , the previous condition on  $g_{ee}$  requires that the Luttinger charge parameter  $K$  lies in the interval  $0.70 \lesssim K \leq 1$ . In the present kind of setup, the value of  $K$  is likely to be above 0.70, due to the screening from the dielectrics and electrodes, as well as from the nearby superconductor. If not,  $K$  can be pushed above 0.70 by adjusting the strength  $g_2$  of the e-e interaction, recalling that  $K \approx (1 + g_2/(\pi v_F))^{-1/2}$  and with the value of  $v_F$  fixed by the condition that  $Q = 2(k_F + q_0)$ . The value of  $g_2$  may be altered by modifying the screening from the dielectrics and metallic electrodes. Focussing on metallic screening, a detailed analysis<sup>74</sup> shows that, to leading order,

$$g_2 \approx \frac{e^2}{\pi \epsilon_0 \epsilon_r} \ln\left(\frac{2d}{\xi}\right), \quad (27)$$

where  $\xi$  is the radius of the quantum wire and  $\epsilon_r$  is the averaged relative permittivity of the dopant and capping layers between the quantum well and the nearest gate, at a distance  $d$  from the wire. Given this, the setup is now to be designed in such a way that the parameters in Eq. (27) produce a value of  $g_2$  corresponding to  $0.70 \lesssim K \leq 1$ , with  $d$  playing the role of a tuning parameter. We should recall that the bosonization formalism constraints the validity of the expression  $K \approx (1 + g_2/(\pi v_F))^{-1/2}$  used above to the weak-coupling limit  $K \approx 1$ . Still, *Bethe Ansatz* and numerical results for this class of models suggest that this expression well captures the effective  $K$ -parameter also for intermediate to strong coupling<sup>75</sup>.

Turning to  $PC_1$ , maximizing the upper bound on  $L_{ins}$  by taking  $L_{sc} \approx 7.6 \mu\text{m}$  (corresponding to  $g_{sc} \approx 2.3 \times 10^{-3}$  with  $g_{ee} \approx -0.20$ ) and taking  $r = 2$  (corresponding to an insulating gap twice as large as the superconducting gap), we obtain that  $L_{ins} \lesssim 3.8 \mu\text{m}$  or, using Eq. (25),  $l_{ins}^* \lesssim 8.9$ . We now search for the lower bound on the bare value of the spin-orbit parameter  $g_{so}$  so that, under RG,  $g_{so}$  approaches unity at a scaling

length  $l_{ins}^* \lesssim 8.9$ . We find  $g_{so} \gtrsim 0.43$ , with a smaller  $g_{ee}$  corresponding to a larger lower bound on  $g_{so}$  (for fixed  $g_{sc}$ ). Therefore, having an InAs wire at  $T \approx 0.1 \text{ K}$  and coupled to an  $s$ -wave superconductor with the currently largest reported experimental proximity effect<sup>69</sup>, the required strength of the modulated Rashba interaction is minimized when  $g_{sc} \approx 2.3 \times 10^{-3}$ ,  $g_{ee} \approx -0.20$  and  $g_{so} \approx 0.43$ , with these estimates placing the parameters inside the  $PWS_2$  regime.

We now use our previous definitions to write  $g_{so} = (2\hbar v)^{-2} \alpha'^2 / [(\alpha/\beta)^2 + 1]$  where  $\alpha = a\gamma_R$ ,  $\beta = a\gamma_D$ ,  $\alpha' = a\gamma'_R$  and  $\hbar v = v_F$ . With  $\alpha/\beta \approx 2$  (drawn from experimental estimates that  $\alpha/\beta$  for a conventionally gated InAs wire is in the range  $[1.6, 2.3]$ <sup>76</sup>),  $g_{so} \gtrsim 0.43$  implies that  $\alpha' \gtrsim 19 \times 10^{-11} \text{ eVm}$ . As a point of reference, this may be compared with data from an InAs quantum well capped by a solid PEO/LiClO<sub>4</sub> electrolyte, where the Rashba coupling was found to change from  $0.4 \times 10^{-11} \text{ eVm}$  to  $2.8 \times 10^{-11} \text{ eVm}$  when tuning a top gate from 0.3 to 0.8 V<sup>77</sup>. Thus, our lower bound on  $\alpha'$  is around seven times larger than the largest experimental value from Ref. 77. However, the same data reveals a Rashba coupling growing almost five times faster than the gate voltage, within the considered range. Supposing the same rate would be maintained in the next voltage injection, a 7-fold boost in  $\alpha'$  would be possible by raising the voltage to around 4 V. Whereas this gives a first estimate, the actual relation between the Rashba coupling energy and the voltage depends on the various microscopic details of the material and setup and, hence, might not be a simple linear one. In any case, the tuning of the Rashba coupling through the amplitude of the modulated electric field is a general feature of the system and can be exploited, possibly in association with other techniques. For example, if the superconducting proximity effect can be improved, allowing for a larger value of  $g_{sc}$  than the one used above, the lower bound on  $g_{so}$  could be reduced. With  $\Delta$  being highly sensitive to the hybridization between the superconductor and the wire, as well as to the zero-momentum surface density of states of the superconductor<sup>5</sup>, the obvious way would be to try to significantly improve the contacting in the device beyond what has so far been achieved in the laboratory for coatings with Nb<sup>69,70</sup> or Al<sup>71</sup>. An assessment to what extent this is a realistic option is beyond the scope of this paper. A maybe simpler alternative is to lower the temperature scale at which an experiment is carried out, with that raising the upper bound on  $L_{ins}$  and, consequently, reducing the lower bound on  $g_{so}$ .

## B. Case study II: Spin-orbit-coupled cold atoms

Observations of  $p$ -wave Feshbach resonances in spin-polarized <sup>40</sup>K and <sup>6</sup>Li atoms<sup>79</sup> have spurred hopes that a  $p$ -wave superfluid of fermionic cold atoms may soon be realized<sup>80-82</sup>. However, the short lifetimes of the  $p$ -wave pairs in experiments<sup>83</sup> make this prospect appear

challenging. Various alternative ways of generating a  $p$ -wave superfluid phase have been proposed, like the one by Zhang *et al.*<sup>84</sup> where an  $s$ -wave Feshbach resonance is combined with an artificial spin-orbit coupling to produce a 2D  $p_x + ip_y$  superfluid. Several other proposals to realize topological phases with cold atoms are discussed in Refs. 7,8,85–89. Could our scheme provide a new vista, now specifically for generating a one-dimensional spinless  $p$ -wave superfluid exhibiting MZMs? While a precise blueprint for an experimental setup is beyond this work, we shall attempt an analysis of the various components that go into it: (i) a repulsively interacting cold gas of fermionic atoms trapped in a 1D optical lattice; (ii) a uniform coupling to Rashba- and Dresselhaus-type spin-orbit fields; (iii) proximity coupling to a reservoir of  $s$ -wave paired fermions; and (iv) a spatially modulated Rashba-type spin-orbit interaction.

As for (i), there are by now a multitude of experimental reports of ultracold gases of fermionic atoms confined to one-dimensional lattices<sup>90</sup>. Experiments on  $^{40}\text{K}$  in a 3D optical lattice<sup>91,92</sup> have shown that the repulsive interaction strength as measured by  $U/t$  (with  $U$  a Hubbard-like on-site coupling and  $t$  a hopping amplitude) can be tuned up to two orders of magnitude, using a magnetically controlled Feshbach resonance. A 1D adaption is expected to yield similar results.

The second element, (ii), is also expected to be within easy reach, given the experimental progress in manufacturing synthetic gauge fields<sup>93</sup>. Specifically, Rashba and Dresselhaus spin-orbit couplings of equal strength can be synthesized in the laboratory from two-photon Raman transitions driven by a pair of laser beams<sup>94</sup>. The technique – with the equal mixture of Rashba and Dresselhaus couplings dictated by symmetry, and known from condensed matter physics as the “persistent spin-helix symmetry point”<sup>95,96</sup> – has been successfully tested with both  $^{40}\text{K}$  and with  $^6\text{Li}$  cold atoms<sup>97,98</sup>.

Turning to (iii), a proximity-type pairing can be engineered via the coupling of the fermions to a BEC bulk reservoir of Feshbach molecules, as discussed in Ref. 8. The coupling between the two systems is here transmitted by a pulsed RF field with a Rabi frequency that sets the scale of the effective proximity pairing.

Finally, considering (iv), we note that a theoretical proposal for emulating a *position-dependent* Rashba-type interaction for atomic BECs has very recently been put forward by Su *et al.*<sup>99</sup>. The scheme relies on cyclically laser coupling internal atomic states in an environment where the detuning from resonance depends on the spatial position. In Ref. 99, transitions between magnetically split hyperfine states in  $^{87}\text{Rb}$  are detuned from two-photon Raman resonance using a spatially inhomogeneous magnetic field. The same scheme is expected to apply for cyclically coupled states in the two hyperfine manifolds of the fermionic alkali atoms  $^6\text{Li}$  and  $^{40}\text{K}$ ,  $F = 1/2, 3/2$  and  $F = 9/2, 7/2$ , respectively, making a realization appear feasible.

With this as a backdrop, let us now check the ex-

pediency of a cold-atom emulation by examining the conditions in Sec. IV. In the present picture, it is convenient to use Eq. (25) to rewrite  $PC_2$  &  $PC_3$  in terms of the dimensionless RG scaling length as  $l_{sc}^* < \min\{\ln(\Lambda/(k_B T)), \ln(N)\}$ . We then take  $T \approx 1$  nK as a typical temperature scale in a cold atom setup and assume  $\Lambda$  to be of the same order of magnitude as the Fermi energy, which, importing data from Ref. 84, gives  $\Lambda \approx \hbar \times 1$  KHz. This yields  $\ln(\Lambda/(k_B T)) \approx 2.0$ , with  $\ln(\Lambda/(k_B T)) < \ln(N)$  for any number of atoms  $N > 8$ . Our task is now to assess the experimental viability of satisfying  $l_{sc}^* \lesssim 2.0$  in the proposed setup.

We start by considering the strength of inter-atomic repulsion which is expected to be tunable via the Feshbach resonance technique mentioned above. In a repulsive fermion realization<sup>91,92</sup>, the predominantly on-site (Hubbard-like) character of the interaction restricts the Luttinger parameter  $K$  to be above  $1/2$ , with  $K = 1/2$  corresponding to an infinitely strong on-site repulsion. We assume a repulsion of intermediary strength and take  $K \approx 0.75$ , corresponding to  $g_{ee} \approx -0.25$ .

We now ask what is the lower bound on the bare  $g_{sc}$  so that its RG flow approaches unity at a length  $l_{sc}^* \lesssim 2.0$  when  $g_{ee} \approx -0.25$ . We find that  $g_{sc} \gtrsim 0.18$ , corresponding to  $\Delta \gtrsim \hbar \times 0.18$  kHz where we have used that  $g_{sc} = \Delta/E_F$ , with the Fermi energy  $E_F = v_F/a \approx \hbar \times 1$  kHz, as before. According to Ref. 8, an order-of-magnitude estimate for the effective pairing energy yields  $\Delta \approx \hbar \times 10$  kHz. Hence our lower bound on  $\Delta$  is far below the typical experimental value.

Coming to  $PC_1$ , this practical criterion can be rewritten through Eq. (25) as  $l_{ins}^* < l_{sc}^* - \ln(r)$ . Taking  $l_{sc}^* \approx 2.0$  (corresponding to  $g_{ee} \approx -0.25$  with  $g_{sc} \approx 0.18$ ) and  $r = 2$ , gives  $l_{ins}^* \lesssim 1.3$ . From the numerics we find that to have  $g_{so}$  reaching unity at an RG length  $l_{ins}^* \lesssim 1.3$ , its bare value must satisfy  $g_{so} \gtrsim 0.78$ , with a larger  $g_{sc}$  corresponding to a larger lower bound on  $g_{so}$  (for fixed  $g_{ee}$ ). The minimal set  $g_{ee} \approx -0.25$ ,  $g_{sc} \approx 0.18$  and  $g_{so} \approx 0.78$  belongs to the  $PWS_2$  regime.

Using the parametrization above, we write  $g_{so} = (2E_F)^{-2} \gamma_R'^2 / [(\gamma_R/\gamma_D)^2 + 1]$ . Applying the numerical estimate  $g_{so} \gtrsim 0.78$ , with  $\gamma_R \approx \gamma_D$  and the same  $E_F$  as before, we estimate that  $\gamma_R' \gtrsim \hbar \times 2.5$  kHz for a working device. From Ref. 84 we learn that the experimental spin-orbit coupling in cold atoms can reach magnitudes up to  $\hbar \times 10$  kHz. Therefore, our required lower bound on  $\gamma_R'$  is well within today’s capabilities. This puts a cold-atom implementation of our scheme safely within the realm of what is possible to achieve in the laboratory.

## VII. SUMMARY

We have proposed and analyzed a magnetic-field-free scheme for synthesizing unpaired Majorana zero modes at the ends of a single-channel quantum wire. The wire is modeled as gated by a periodic array of charged top gates, supporting Rashba, Dresselhaus, and e-e interac-

tions, and proximity-coupled to an  $s$ -wave superconductor which induces a topological  $p$ -wave superconducting phase.

The microscopic Hamiltonian which describes the proximity-coupled quantum wire is cast in a low-energy bosonized form that is treated using a renormalization group approach. This formalism allows us to derive the RG flow equations of the theory and obtain the phase diagram of the system. Adding “practical” limits (determined by temperature and by the size of the system) on the RG length scales, we extract the conditions for a working device in the laboratory.

Estimates based on a case study of an InAs wire, well contacted to a Nb or Al  $s$ -wave superconductor, indicates that a realization of our scheme in a hybrid semiconductor-superconductor device requires improvements upon present-day materials and design capabilities. As transpires from our analysis, however, the required improvements may well be within reach of near-future developments in quantum device engineering. Indeed, having an all-electric device for synthesizing unpaired Majorana zero modes would be an important step towards applications in topological quantum computing.

A variant of our scheme where spin-orbit-coupled

ultracold fermionic atoms trapped in an optical lattice are effectively proximity-coupled to a BEC reservoir of Feshbach molecules may provide a more easily accessible platform, at least for now. While there already exists a large number of proposals for synthesizing Majorana zero modes using cold fermionic atoms<sup>7,8,85–89</sup>, ours is distinguished by taking advantage of a Feshbach-generated repulsive interaction between the atoms. Its realization would be fascinating, opening up an experimental window on how to drive a topological quantum phase transition (from  $s$ -wave pairing to spinless  $p$ -wave pairing) by tuning the strength of an effective fermion interaction.

**Acknowledgements** We thank E. Ardonne, K. Le Hur, P. Sacramento, A. Tagliacozzo, H.-Q. Xu, and F. Zhang for valuable input. H.J. acknowledges hospitality at CPTH at École Polytechnique where part of this work was carried out. This research was supported by CNPq and CAPES (M.M.), Georgian National Science Foundation and Science and Technology Center in Ukraine through the joint grant No. STCU-5893 (G.J.), and the Swedish Research Council and STINT (H.J.)

- 
- <sup>1</sup> For a review, see F. Wilczek, Nat. Phys. **5**, 614 (2009).
  - <sup>2</sup> C. Chamon, R. Jackiw, Y. Nishida, S.-Y. Pi, and L. Santos, Phys. Rev. B **81**, 224515 (2010).
  - <sup>3</sup> C. W. J. Beenakker, Phys. Rev. Lett. **112**, 070604 (2014).
  - <sup>4</sup> C. Nayak, S. H. Simon, A. Stern, M. Freedman, and S. Das Sarma, Rev. Mod. Phys. **80**, 1083 (2008).
  - <sup>5</sup> For a review, see J. Alicea, Rep. Prog. Phys. **75**, 076501 (2012).
  - <sup>6</sup> G. Moore and N. Read, Nucl. Phys. B **360**, 362 (1991).
  - <sup>7</sup> M. Sato, Y. Takahashi, and S. Fujimoto, Phys. Rev. Lett. **103**, 020401 (2009).
  - <sup>8</sup> L. Jiang, T. Kitagawa, J. Alicea, A. R. Akhmerov, D. Pekker, G. Refael, J. I. Cirac, E. Demler, M. D. Lukin, and P. Zoller, Phys. Rev. Lett. **106**, 220402 (2011).
  - <sup>9</sup> A. Y. Kitaev, Phys. Usp. **44**, 131 (2001).
  - <sup>10</sup> N. Read and D. Green, Phys. Rev. B **61**, 10267 (2000).
  - <sup>11</sup> D. A. Ivanov, Phys. Rev. Lett. **86**, 268 (2001).
  - <sup>12</sup> L. Fu and C. L. Kane, Phys. Rev. Lett. **100**, 096407 (2008).
  - <sup>13</sup> R. M. Lutchyn, J. D. Sau, and S. DasSarma, Phys. Rev. Lett., **105**, 077001 (2010).
  - <sup>14</sup> Y. Oreg, G. Refael, and F. von Oppen, Phys. Rev. Lett. **105**, 177002 (2010).
  - <sup>15</sup> S. Nadj-Perge, I.K. Drozdov, B.A. Bernevig, and A. Yazdani, Phys. Rev. B **88**, 020407(R) (2013).
  - <sup>16</sup> For the experimental status up to January 2015, see S. Das Sarma, M. Freedman, and C. Nayak, arXiv:1501.02813v2.
  - <sup>17</sup> J. Alicea, Y. Oreg, G. Refael, F. von Oppen, and M. P. A. Fisher, Nat. Phys. **7**, 412 (2011).
  - <sup>18</sup> E. M. Stoudenmire, J. Alicea, O. A. Starykh, and M. P. A. Fisher, Phys. Rev. B **84**, 014503 (2011).
  - <sup>19</sup> A. C. Potter and P. A. Lee, Phys. Rev. B **83**, 184520 (2011),
  - <sup>20</sup> J. D. Sau, S. Tewari, and S. Das Sarma, Phys. Rev. B **85**, 064512 (2012).
  - <sup>21</sup> M. A. Nielsen and I. L. Chuang, *Quantum Computation and Quantum Information* (Cambridge University Press, 2011).
  - <sup>22</sup> S. Bravyi and A. Kitaev, Phys. Rev. A **71**, 022316 (2005).
  - <sup>23</sup> S. Bravyi, Phys. Rev. A **73**, 042313 (2006).
  - <sup>24</sup> D. I. Pikulin, T. Hyart, S. Mi, J. Tworzydło, M. Wimmer, and C. W. J. Beenakker, Phys. Rev. B **89**, 161403(R) (2014).
  - <sup>25</sup> D. Awschalom and N. Samarth, Physics **2**, 50 (2009).
  - <sup>26</sup> C. L. M. Wong and K. T. Law, Phys. Rev. B **86**, 184516 (2012).
  - <sup>27</sup> F. Zhang, C. L. Kane, and E. J. Mele, Phys. Rev. Lett. **111**, 056402 (2013).
  - <sup>28</sup> S. Nakosai, J. C. Budich, Y. Tanaka, B. Trauzettel, and N. Nagaosa, Phys. Rev. Lett. **110**, 117002 (2013).
  - <sup>29</sup> E. Gaidamauskas, J. Paaske, and K. Flensberg, Phys. Rev. Lett. **112**, 126402 (2014).
  - <sup>30</sup> S. B. Chung, J. Horowitz, and X.-L. Qi, Phys. Rev. B **88**, 214514 (2013).
  - <sup>31</sup> S. Deng, L. Viola, and G. Ortiz, Phys. Rev. Lett. **108**, 036803 (2012).
  - <sup>32</sup> A. Keselman, L. Fu, A. Stern, and E. Berg, Phys. Rev. Lett. **111**, 116402 (2013).
  - <sup>33</sup> D. Sticlet, C. Bena, and P. Simon, Phys. Rev. B **87**, 104509 (2013).
  - <sup>34</sup> X.-J. Liu, C. L. M. Wong, and K. T. Law, Phys. Rev. X **4**, 021018 (2014).
  - <sup>35</sup> E. Dumitrescu, J. D. Sau, and S. Tewari, Phys. Rev. B **90**, 245438 (2014).
  - <sup>36</sup> A. Haim, A. Keselman, E. Berg, and Y. Oreg, Phys. Rev. B **89**, 220504 (2014).
  - <sup>37</sup> J. Klinovaja and D. Loss, Phys. Rev. B **90**, 045118 (2014).

- <sup>38</sup> P. Kotetes, Phys. Rev. B **92**, 014514 (2015).
- <sup>39</sup> A. P. Schnyder, S. Ryu, A. Furusaki and A. W. W. Ludwig, Phys. Rev. B **78**, 195125 (2008).
- <sup>40</sup> A. Kitaev, AIP Conference Proceedings **1134**, 22 (American Institute of Physics, New York, 2009).
- <sup>41</sup> For a review, see P. Kotetes, New J. Phys. **15**, 105027 (2013).
- <sup>42</sup> A. A. Reynoso and D. Frustaglia, Phys. Rev. B **87**, 115420 (2013).
- <sup>43</sup> G. I. Japaridze, H. Johannesson, and M. Malard, Phys. Rev. B **89**, 201403(R) (2014).
- <sup>44</sup> C. Wu, B. A. Bernevig, and S.-C. Zhang, Phys. Rev. Lett. **96**, 106401 (2006).
- <sup>45</sup> C. Xu and J. E. Moore, Phys. Rev. B **73**, 045322 (2006).
- <sup>46</sup> M. Malard, I. Grusha, G. I. Japaridze, and H. Johannesson, Phys. Rev. B **84**, 075466 (2011).
- <sup>47</sup> E. Ya. Sherman, Phys. Rev. B **67**, 161303(R) (2003).
- <sup>48</sup> L. E. Golub and E. L. Ivchenko, Phys. Rev. B **69**, 115333 (2004).
- <sup>49</sup> L. Fu, Phys. Rev. Lett. **104**, 056402 (2010).
- <sup>50</sup> S. Tewari and J. D. Sau, Phys. Rev. Lett. **109**, 150408 (2012).
- <sup>51</sup> T. Giamarchi, *Quantum Physics in One Dimension* (Oxford University Press, Oxford, 2004).
- <sup>52</sup> A. Schulz, A. De Martino, P. Ingenhoven, and R. Egger, Phys. Rev. B **79**, 205432 (2009).
- <sup>53</sup> For a review, see M. Malard, Braz. J. Phys. **43**, 182 (2013).
- <sup>54</sup> For a review, see M. König, H. Buhmann, L. W. Molenkamp, T. Hughes, C.-X. Liu, X.-L. Qi, and S.-C. Zhang, J. Phys. Soc. Jpn. **77**, 031007 (2008).
- <sup>55</sup> B. Braunecker, A. Ström, and G. I. Japaridze, Phys. Rev. B **87**, 075151 (2013).
- <sup>56</sup> J.V. Jose, L.P. Kadanoff, S. Kirkpatrick, and D.R. Nelson, Phys. Rev. B **16**, 1217 (1977).
- <sup>57</sup> D. Boyanovsky, J. Phys. A: Math. Gen. **22**, 2601 (1989).
- <sup>58</sup> P. Lecheminant, A. O. Gogolin, A. A. Nersesyan, Nucl. Phys. B **639**, 502 (2002).
- <sup>59</sup> A. O. Gogolin, A. A. Nersesyan, and A. M. Tsvelik, *Bosonization and Strongly Correlated Systems*, Cambridge University Press (1998).
- <sup>60</sup> C. Spänslätt, E. Ardonne, J. C. Budich, and T. H. Hansson, J. Phys. C **27**, 405701 (2015).
- <sup>61</sup> N. Kainaris and S. T. Carr, Phys. Rev. B **92**, 035139 (2015).
- <sup>62</sup> E. Sela, A. Altland, and A. Rosch, Phys. Rev. B **84**, 085114 (2011).
- <sup>63</sup> S. Gangadharaiah, B. Braunecker, P. Simon, and D. Loss, Phys. Rev. Lett. **107**, 036801 (2011).
- <sup>64</sup> J. C. Budich and E. Ardonne, Phys. Rev. B **88**, 075419 (2013).
- <sup>65</sup> A. M. Turner, F. Pollmann, and E. Berg, Phys. Rev. B **83**, 075102 (2011).
- <sup>66</sup> L. Fidkowski and A. Kitaev, Phys. Rev. B **83**, 075103 (2011).
- <sup>67</sup> A. Altland and M. R. Zirnbauer, Phys. Rev. B **55**, 1142 (1997).
- <sup>68</sup> P. Bhattacharaya, *Properties of lattice-matched and strained indium gallium arsenide* (EMIS Datareview Series No. 8, Stevenage, UK).
- <sup>69</sup> V. Mourik, K. Zuo, S. M. Frolov, S. R. Plissard, E. P. A. M. Bakkers, and L. P. Kouwenhoven, Science **336**, 1003 (2012).
- <sup>70</sup> M. T. Deng, C. L. Yu, G. Y. Huang, M. Larsson, P. Caroff, and H. Q. Xu, Nano Lett. **12**, 6414 (2012).
- <sup>71</sup> W. Chang, S. M. Albrecht, T. S. Jespersen, F. Kuemmeth, P. Krogstrup, J. Nygård, and C. M. Marcus, Nat. Nanotech. **10**, 232 (2015).
- <sup>72</sup> D. Liu and S. Das Sarma, Phys. Rev. B **51**, 13821 (1995).
- <sup>73</sup> H. J. Joyce, C. J. Docherty, Q. Gao, H. T. Tan, C. Jagadish, J. Lloyd-Hughes, L. M. Herz, and M. B. Johnston, Nanotechnology **24**, 214006 (2013).
- <sup>74</sup> K. Byczuk and T. Dietl, Phys. Rev. B **60**, 1507 (1999).
- <sup>75</sup> H. J. Schulz, Int. J. Mod. Phys. B **5**, 57 (1991).
- <sup>76</sup> S. Giglberger, L. E. Golub, V. V. Belkov, S. N. Danilov, D. Schuh, Ch. Gerl, F. Rohlfing, J. Stahl, W. Wegscheider, D. Weiss, W. Prettl, and S.D. Ganichev, Phys. Rev. B **75**, 035327 (2007).
- <sup>77</sup> D. Liang and X. P. A. Gao, Nano Lett. **6**, 3263 (2012).
- <sup>78</sup> M. Hashimoto, I. M. Vishik, R.-H. He, T. P. Devereaux, and Z.-X. Shen, Nature Phys. **10**, 483 (2014).
- <sup>79</sup> C. A. Regal, C. Ticknor, J. L. Bohn, and D. S. Jin, Phys. Rev. Lett. **90**, 053201 (2003).
- <sup>80</sup> S. S. Botelho and C. A. R. Sa de Melo, J. Low Temp. Phys. **140**, 409 (2005).
- <sup>81</sup> V. Gurarie, L. Radzihovsky, and A. V. Andreev, Phys. Rev. Lett. **94**, 230403 (2005).
- <sup>82</sup> C.-H. Cheng and S.-K. Yip, Phys. Rev. Lett. **95**, 070404 (2005).
- <sup>83</sup> J. P. Gaebler, J. T. Stewart, J. L. Bohn, and D. S. Jin, Phys. Rev. Lett. **98**, 200403 (2007).
- <sup>84</sup> C. Zhang, S. Tewari, R. M. Lutchyn, and S. Das Sarma, Phys. Rev. Lett. **101**, 160401 (2008).
- <sup>85</sup> N. Goldman, I. Satija, P. Nikolic, A. Bermudez, M. A. Martin-Delgado, M. Lewenstein, and I. B. Spielman, Phys. Rev. Lett. **105**, 255302 (2010).
- <sup>86</sup> T. D. Stanescu, V. Galitski, and S. Das Sarma, Phys. Rev. A **82**, 013608 (2010).
- <sup>87</sup> J. Levinsen, N. R. Cooper, and G. V. Shlyapnikov, Phys. Rev. A, **84**, 013603 (2011).
- <sup>88</sup> K. Sun, Z. Gu, H. Katsura, and S. Das Sarma, Phys. Rev. Lett. **106**, 236803 (2011).
- <sup>89</sup> S. Diehl, E. Rico, M. A. Baranov, and P. Zoller, Nat. Phys. **7**, 971 (2011).
- <sup>90</sup> For an overview, see X.-W. Guan, M. T. Batchelor, and C. Lee, Rev. Mod. Phys. **85**, 1633 (2013).
- <sup>91</sup> R. Jördens, N. Strohmaier, K. Günter, H. Moritz, and T. Esslinger, Nature **455**, 204 (2008).
- <sup>92</sup> U. Schneider, L. Hackermüller, S. Will, Th. Best, I. Bloch, T. A. Costi, R. W. Helmes, D. Rasch, and A. Rosch, Science **322**, 1520 (2008).
- <sup>93</sup> For a review, see N. Goldman, G. Juzeliūnas, P. Öhberg, and I. B. Spielman, Rep. Prog. Phys. **77**, 126401 (2014).
- <sup>94</sup> For a review, see V. Galitski and I. B. Spielman, Nature **494**, 49 (2013).
- <sup>95</sup> B. A. Bernevig, J. Orenstein, and S.-C. Zhang, Phys. Rev. Lett. **97**, 236601 (2006).
- <sup>96</sup> D. F. Mross and H. Johannesson, Phys. Rev. B **80**, 155302 (2009).
- <sup>97</sup> P. Wang, Z.-Q. Yu, Z. Fu, J. Miao, L. Huang, S. Chai, H. Zhai, and J. Zhang Phys. Rev. Lett. **109**, 095301 (2012).
- <sup>98</sup> L. W. Cheuk, A. T. Sommer, Z. Hadzibabic, T. Yefsah, W. S. Bakr, and M. W. Zwierlein, Phys. Rev. Lett. **109**, 095302 (2012).
- <sup>99</sup> S.-W. Su, S.-C. Gou, I.-K. Liu, I. B. Spielman, L. Santos, A. Acus, A. Mekys, J. Ruseckas, and G. Juzeliūnas, New J. Phys. **17**, 033045 (2015).